Progress In Electromagnetics Research B, Vol. 85, 85–101, 2019

Design and Optimization of Structure of Tower-Type Coil in Wireless Charging System for Electric Vehicles

Zhongqi Li[1], Min Zhang[1], Shoudao Huang[2], and Jiliang Yi[1, *]

Abstract—Magnetic resonant wireless power transfer (WPT) is an emerging technology that may create new applications for wireless power charging. However, the output voltage and efficiency fluctuations resulting from lateral misalignments are main obstructing factors for promoting this technology. In this paper, a structure of tower-type coils is proposed. The mathematical model of the proposed structure is built based on equivalent circuit method. The expressions of the output voltage and efficiency are then derived by solving the system equivalent equations. In addition, a method of optimizing the mutual inductance between the transmission coil and intermediate coil and the strong-coupling parameters between the intermediate coil and receiving coil is proposed. The mutual inductance between the transmission coil and intermediate coil can be kept nearly constant with lateral misalignments, and the optimum strong-coupling parameter between the intermediate coil and the receiving coil can be obtained by the proposed method. Therefore, the output voltage and efficiency can be kept nearly constant with different lateral misalignments. The WPT system based on tower-type coils via magnetic resonance coupling is designed. Simulated and experimental results validating the proposed method are given.

1. INTRODUCTION

Electric vehicles (EVs) are receiving increasing attention in the international research community due to tougher regulations triggered by environment and energy security concerns. There are two charging modes for electric vehicles, including wired charging mode and wireless charging mode [1–4]. Compared to the wired charging mode of EVs, the convenience of wireless charging using magnetic resonance can make EVs more acceptable to drivers because they do not need to handle power plug. At the same time, EVs system using wireless charging mode can be safer [5–7].

Two conditions should be satisfied in a magnetic resonant wireless charging system to maintain the stability of a system [8]. First, the system efficiency is high [9]. Secondly, the output voltage or output current of the system is nearly constant. However, in practice, inevitable lateral and vertical misalignments between the transmission coil and receiving coil lead to variations of the mutual inductance between the transmission coil and receiving coil [10]. The efficiency is decreased, and the output voltage or output current may be changed as the mutual inductance between the transmission coil and receiving coil is changed [11]. The system efficiency was improved by adjusting equivalent load resistance with lateral and vertical misalignments [12]. The constant output voltage was also obtained by adjusting equivalent load resistance. However, the equivalent load resistance at maximum efficiency is not the same as that at constant output voltage for a given mutual inductance [13, 14]. In order to achieve simultaneously high efficiency and constant output voltage for a wireless charging system, a maximum efficiency point tracking control scheme was proposed to maximize system efficiency [15].

Received 12 May 2019, Accepted 26 July 2019, Scheduled 14 August 2019

* Corresponding author: Jiliang Yi (ieee_china@126.com).

[1] College of Traffic Engineering, Hunan University of Technology, Zhuzhou 412007, China. [2] College of Electrical and Information Engineering, Hunan University, Changsha 410082, China.

When the mutual inductance between the transmission coil and receiving coil is changed, the minimum DC input current can be tracked by real-time changing the duty cycle of the DC-DC converter (The minimum input current is an equivalent condition of the maximum efficiency when the input voltage and output voltage are kept constant). The output voltage is kept constant by changing the duty cycle of another DC-DC converter. However, two DC-DC converters are added to the wireless charging systems, and the system efficiency is decreased inevitably because two DC-DC converters have power losses. At the same time, it is difficult to track input current because the waveform of the input current is not standard.

There are other methods using new coil structures to deal with the adverse effect of misalignments on the efficiency and output voltage: 1) A narrow-width I-type power supply rail and pickups were proposed [16]. The experimental results showed that the output power was reduced and reached nearly 1 kW at the cross-point of the poles as the pickup moved away from the center of the pole along X-direction, and the output power exceeded 20 kW as the pickup laterally moved in Y-direction within 20 cm and became half at 24 cm from the center of the power supply rail. The system efficiency was 74%; 2) A large lateral displacement of 30 cm at an air gap of 20 cm was experimentally obtained by using ultraslim S-type power supply rails [17]. The load power reached the -3 dB point having half of its maximum load power with the lateral tolerance of 30 cm; 3) A new homogeneous WPT technique was proposed and implemented to maintain the output voltage constant for lateral and vertical misalignments systems [18, 19]. The homogeneous magnetic field should be paid with reduction of the quality factor of the transmitter because the transmitter is composed of many small coils (58 mm $\times$ 58 mm $\times$ 22.5 mm) [19]. The system efficiency is reduced when the quality factor of the transmitter is decreased [18]; 4) Reference [20] proposed an extremely asymmetric coil structure, including a big power supply coil set (110 cm $\times$ 80 cm) and a small pick-up coil set. When the pick-up coil laterally deviated from the center of the power supply coil by 39 cm, the output voltage was reduced by about 29% from the maximum output voltage 150 V. In conclusion, it is necessary to further reduce output voltage pulsations and improve the efficiency for electric vehicles. In this paper, the structure of tower-type coils is proposed to reduce output voltage pulsations and improve the efficiency.

The remainder of the paper is outlined as follows. Section 2 gives the method of parameters calculated. Section 3 describes the two-coil WPT system. Section 4 proposes the structure of tower-type coils and builds the model of the proposed structure. Section 5 proposes a method of optimization parameters. Section 6 presents the experimental setup and the measurement results with lateral misalignments between the transmission coil and receiving coil. Section 7 draws the conclusion.

2. PARAMETERS CALCULATED

2.1. Calculated Mutual Inductance and Self-Inductance

Figure 1 shows two loops with lateral misalignments between loop_1 and loop_2. D is the transmission distance, a the radius of loop_1, b the radius of loop_2, and Δ the lateral misalignments between loop_1 and loop_2.

The mutual inductance and self-inductance of two loops whose axes are parallel can be expressed by the single integral [21–23]

$$Mu(a,b,\Delta,D) = \pi\mu_0\sqrt{ab}\int_0^\infty J_1\left(x\sqrt{a/b}\right)J_1\left(x\sqrt{a/b}\right)\times J_0\left(x\frac{\Delta}{\sqrt{ab}}\right)\exp\left(-x\frac{D}{\sqrt{ab}}\right)dx \quad (1)$$

$$L(a,r) = \mu_0 a\left(\ln\left(\frac{8a}{r}\right)-2\right) \quad (2)$$

where J_0 and J_1 are the Bessel functions of zeroth-order and first-order, respectively. r is the radius of the copper. μ_0 is the magnetic conductivity.

For a coil composed of multi-turn, the mutual inductance between the transmission coil and receiving coil can be calculated using

$$M_{ab} = \sum_{i=1}^{N_A}\sum_{j=1}^{N_B} Mu(a_i,b_j,D,\Delta) \quad (3)$$

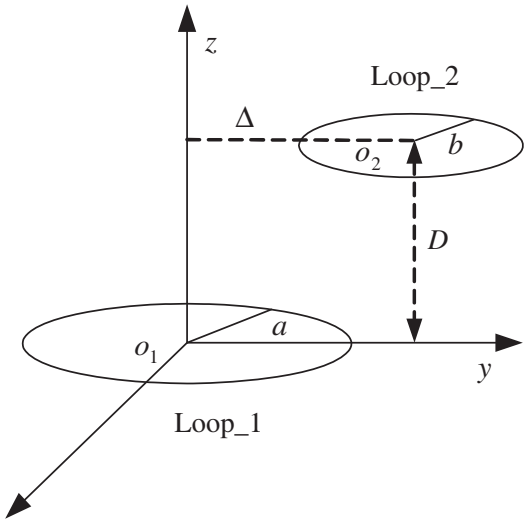

Figure 1. Lateral misalignments between loop_1 and loop_2.

where N_A and a_i are the number of turns of the transmission coil and the radius of the transmission coil, respectively. N_B and b_j are the number of turns of the receiving coil and the radius of the receiving coil, respectively.

A multi-turn planar spiral coil can be approximately equivalent to the sum of a plurality of coaxial single-turn coils. Self-inductance of each coil can be calculated by Eq. (4).

$$L_a = \sum_{i=1}^{N_A} L\left(a_i, r\right) + \sum_{i=1}^{N_A}\sum_{j=1}^{N_A} Mu\left(a_i, a_j, D=0, \Delta=0\right)\left(1-\delta_{i,j}\right) \tag{4}$$

where $\delta_{i,j} = 1$ with $i = j$ or $\delta_{i,j} = 0$ with $i \neq j$.

The coupling coefficient between each coil is defined as follows:

$$k_{ab} = \frac{M_{ab}}{\sqrt{L_a L_b}}, \quad 0 \leq k_{ab} \leq 1 \tag{5}$$

As shown in Eqs. (1) and (3), it can be seen that mutual inductance is dependent on a, b, D, and Δ. When a, b, and D are fixed, mutual inductance is only related to Δ. The bigger the value of Δ is, the smaller the mutual inductance becomes, and the coupling coefficient k_{ab} is decreased according to Eq. (5).

2.2. Calculated Resistance

The resistance of each coil is calculated as follows [24]:

$$\begin{aligned} R \;=\; & R_{dc\_\mathrm{strand}} + R_{ac\_\mathrm{strand}}/n_s - R_{dc\_\mathrm{strand}}\frac{\beta\gamma_s}{2}\frac{ber_2(\gamma_s)ber'(\gamma_s) + bei_2(\gamma_s)bei'(\gamma_s)}{ber^2(\gamma_s) + bei^2(\gamma_s)} \\ & + \sum_{i=1}^{N} n_s S_{av\_i} G_{\mathrm{strand}} h_{ext\_i}^2 \end{aligned} \tag{6}$$

where

$$\begin{aligned} R_{ac\_\mathrm{strand}} \;&=\; R_{dc\_\mathrm{strand}}\frac{\gamma_s}{2}\frac{ber(\gamma_s)bei'(\gamma_s) - bei(\gamma_s)ber'(\gamma_s)}{ber'^2(\gamma_s) + bei'^2(\gamma_s)} \\ G_{\mathrm{strand}} \;&=\; -\frac{2\pi\gamma_s}{\delta}\frac{ber_2(\gamma_s)ber'(\gamma_s) + bei_2(\gamma_s)bei'(\gamma_s)}{ber^2(\gamma_s) + bei^2(\gamma_s)} \end{aligned}$$

h_{ext_i} is the magnetic field generated over the ith-turn of the coil when an RMS current of 1 A is in it. $\gamma_s = 1.414r_s/\delta$, δ is the skin depth, r_s the Litz-wire strand radius, and R_{dc_strand} the DC resistance of the strand. ber, bei, ber', bei' are the Kelvin functions, and ber_2, bei_2 are the second order of Kelvin functions. S_{av} is the average length of the coil. n_s is the number of strands of the Litz-wire.

3. PROPOSED STRUCTURE

3.1. Structure of Tower-Type Coils

In this section, a structure of tower-type coils is proposed to deal with the effect of lateral misalignments on mutual inductance. The proposed structure contains three coils, which are transmission coil, intermediate coil, and receiving coil, labeled as Tx, Im, and Rx, as shown in Fig. 2(a). Im and Rx can be placed on the same plane, or Rx can be placed on the plane staying away from Tx. D is the transmission distance between the Tx and Im. k_{ij} is the coupling coefficient between i-th coil and j-th coil ($i \neq j$; $i, j = 1, 2, 3$). Subscript 1 denotes Tx; subscript 2 denotes Im; subscript 3 denotes Rx. The transmission coil is bigger than the intermediate coil in size, and the intermediate coil is bigger than the receiving coil. k_{13} is smaller than k_{12} because the intermediate coil is bigger than the receiving coil. Therefore, k_{13} may be neglected in the next analysis.

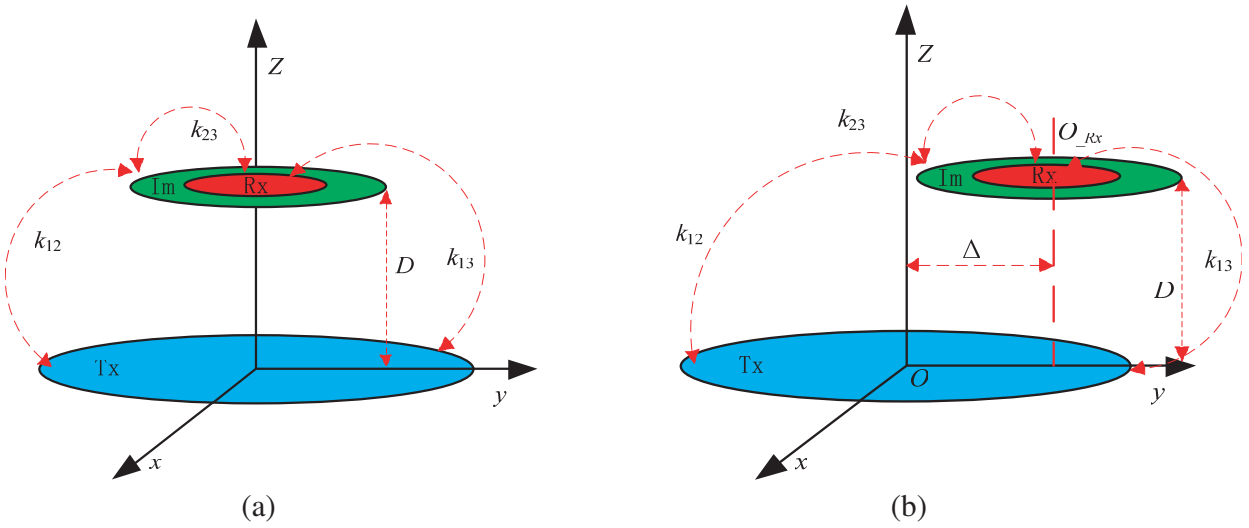

Figure 2. The proposed structure. (a) Structure of tower-type coils. (b) Structure of tower-type coils with misalignment.

Figure 2(b) shows the proposed structure with misalignments. Δ is the lateral misalignments between Tx and Im. In general, the variations of Δ may result in the changes of mutual inductance or the coupling coefficient. However, the variations of the mutual inductances between the Tx and Im are very smooth with misalignments when the proposed structure is used. The system can maintain high efficiency and constant output voltage because mutual inductances between the Tx and Im are nearly constant with misalignments. In Section 3, how to maintain the mutual inductance constant will be further discussed. The overall structure of the proposed structure is shown in Fig. 3. It is composed of a power, Tx , Im, Rx, and Load. C_i is the resonance capacitor ($i = 1, 2, 3$). The main flow of power is as follows: First, the power source via the compensation capacitor C_1 is connected in series to the transmission coil Tx. Secondly, the power is transferred from Tx to Im using magnetic fields. And the power is transferred from Im to Rx. Finally, the power is transferred from Rx to the Load.

The proposed WPT system can be represented in terms of lumped circuit elements (L, C, M, and R), as shown in Fig. 4. R_1 is the parasitic resistance of Tx, R_2 the parasitic resistance of Im, R_3 the parasitic resistance of Rx, R_s the internal resistance of the power source, R_L the load resistance, L_1 the inductance of Tx, L_2 the inductance of Im, L_3 the inductance of Rx, C_1 the external compensating

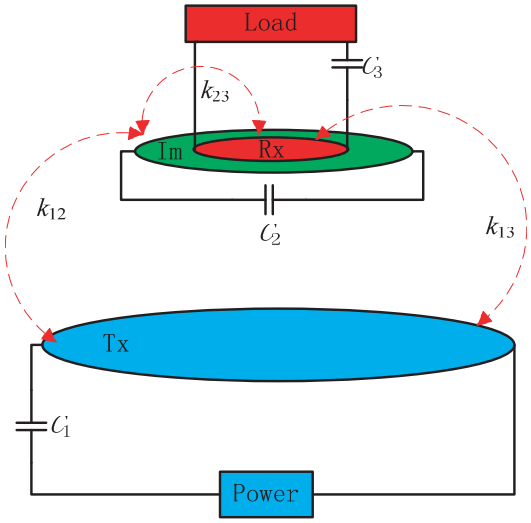

Figure 3. The overall structure of the proposed structure.

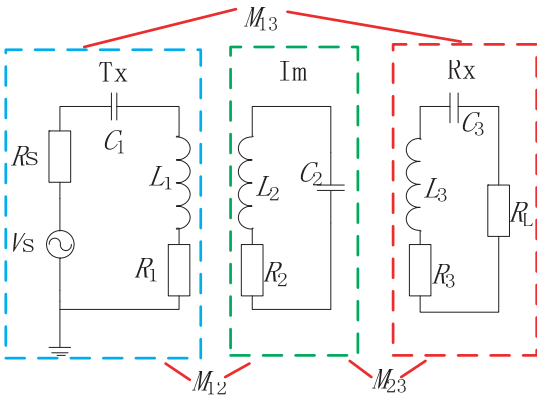

Figure 4. The equivalent circuit model for the WPT system. Each coil is modeled as series resonators.

capacitance of Tx, C_2 the external compensating capacitance of Im, C_3 the external compensating capacitance of Rx, M_{12} the mutual inductance between Tx and Im, M_{13} the mutual inductance between Tx and Rx, M_{23} the mutual inductance between Im and Rx, V_s the voltage of the power, and V_{out} the voltage of the load.

3.2. Mathematical Model of Proposed Structure

By applying Kirchhoff's voltage law (KVL), the proposed WPT system is presented as follows:

$$\begin{cases} Z_1 I_1 + j\omega M_{12} I_2 + j\omega M_{13} I_3 = V_s \\ j\omega M_{12} I_1 + Z_2 I_2 + j\omega M_{23} I_3 = 0 \\ j\omega M_{13} I_1 + j\omega M_{23} I_2 + Z_3 I_3 = 0 \end{cases} \tag{7}$$

$$\begin{cases} Z_1 = R_1 + R_s + j\omega L_1 + 1/(j\omega C_1) \\ Z_2 = R_2 + j\omega L_2 + 1/(j\omega C_2) \\ Z_3 = R_3 + R_L + j\omega L_3 + 1/(j\omega C_3) \end{cases} \tag{8}$$

The current expressions of each coil can be obtained by solving Eqs. (7) and (8)

$$\begin{cases} I_1 = \dfrac{M_{23}^2\omega^2 V_s + Z_2 Z_3 V_s}{\omega^2 M_{12}^2 Z_3 + \omega^2 M_{13}^2 Z_2 + \omega^2 M_{23}^2 Z_1 + Z_1 Z_2 Z_3 - 2j\omega^3 M_{12} M_{23} M_{13}} \\ I_2 = -\dfrac{\omega^2 M_{13} M_{23} V_s + j\omega M_{12} Z_3 V_s}{\omega^2 M_{12}^2 Z_3 + \omega^2 M_{13}^2 Z_2 + \omega^2 M_{23}^2 Z_1 + Z_1 Z_2 Z_3 - 2j\omega^3 M_{12} M_{23} M_{13}} \\ I_3 = -\dfrac{\omega^2 M_{12} M_{23} V_s + j\omega M_{13} Z_2 V_s}{\omega^2 M_{12}^2 Z_3 + \omega^2 M_{13}^2 Z_2 + \omega^2 M_{23}^2 Z_1 + Z_1 Z_2 Z_3 - 2j\omega^3 M_{12} M_{23} M_{13}} \end{cases} \tag{9}$$

where I_1 is the current of Tx, I_2 the current of Im, and I_3 the current of Rx.

According to Eq. (9), the output voltage V_L is as follows:

$$V_L = I_3 R_L = -\frac{\left(\omega^2 M_{12} M_{23} V_s + j\omega M_{13} Z_2 V_s\right) R_L}{\omega^2 M_{12}^2 Z_3 + \omega^2 M_{13}^2 Z_2 + \omega^2 M_{23}^2 Z_1 + Z_1 Z_2 Z_3 - 2j\omega^3 M_{12} M_{23} M_{13}} \tag{10}$$

According to Eqs. (7)–(10), the transmission efficiency is as follows:

$$\eta = \left|\frac{I_3^2 R_L}{V_S I_1}\right| = \left|\frac{(\omega^2 M_{12} M_{23} + j\omega M_{13} Z_2)^2 R_L}{(\omega^2 M_{23}^2 + Z_2 Z_3)(\omega^2 M_{12}^2 Z_3 + \omega^2 M_{13}^2 Z_2 + \omega^2 M_{23}^2 Z_1 + Z_1 Z_2 Z_3 - 2j\omega^3 M_{12} M_{23} M_{13})}\right| \tag{11}$$

When the M_{12} is changed, according to Eq. (10) the output voltage can be obtained, and the transmission efficiency can be obtained according to Eq. (11).

Assuming the frequency of each coil is the same, the efficiency expression (11) and output voltage expression (10) can be simplified as follows:

$$\eta = \frac{(U_1 U_2 + jU_3)^2 U_L}{(U_2^2 + U_L + 1)(U_1^2(1 + U_L) + U_2^2(1 + U_s) + U_3^2 + (1 + U_s)(1 + U_L) - 2jU_1 U_2 U_3)} \tag{12}$$

$$V_L = \frac{(U_1 U_2 + jU_3) V_s U_L}{U_1^2(1 + U_L) + U_3^2 + U_2^2(1 + U_s) + (1 + U_s)(1 + U_L) - 2jU_1 U_2 U_3} \sqrt{R_3/R_1} \tag{13}$$

where the source matching factor is defined as $U_s = R_s/R_1$, the load matching factor defined as $U_L = R_L/R_3$, the strong-coupling parameter between Tx and Im defined as $U_1 = k_{12}(Q_1 Q_2)^{1/2}$, the strong-coupling parameter between Im and Rx defined as $U_2 = k_{23}(Q_2 Q_3)^{1/2}$, the strong-coupling parameter between Tx and Rx defined as $U_3 = k_{13}(Q_1 Q_3)^{1/2}$, the unload quality factor of the Tx coil defined as $Q_1 = \omega L_1/R_1$, the unload quality factor of the Im coil defined as $Q_2 = \omega L_2/R_2$, and the unload quality factor of the Rx coil defined as $Q_3 = \omega L_3/R_3$.

When the coupling coefficient k_{13} is neglected, the efficiency expression (12) and output expression (13) can be simplified as follows:

$$\eta = \frac{(U_1 U_2)^2 U_L}{(U_2^2 + U_L + 1)(U_1^2(1 + U_L) + U_2^2(1 + U_s) + (1 + U_s)(1 + U_L))} \tag{14}$$

$$V_L = \frac{U_1 U_2 U_L V_s}{U_1^2(1 + U_L) + U_2^2(1 + U_s) + (1 + U_s)(1 + U_L)} \sqrt{R_3/R_1} \tag{15}$$

According to Eqs. (14) and (15), the efficiency and output voltage are dependent on U_1, U_2, U_s, and U_L. In general, U_s and U_L are nearly constant for a given load resistance and parameters of Tx ,Im, and Rx coil; therefore, U_1 and U_2 are key parameters to obtain high efficiency and maintain output voltage constant.

By differentiating η with respect to U_2 and equating the differential function to zero

$$\frac{\partial \eta}{\partial U_2} = 0 \tag{16}$$

The optimum strong-coupling parameter between Im and Rx for the optimum efficiency can be obtained as follows:

$$U_{2\_opt} = \left(\frac{2U_L + U_s + 2U_L U + 2U_1^2 U_L + U_L^2 U_s + U_1^2 + U_L^2 + U_1^2 U_L^2 + 1}{U_s + 1}\right)^{\frac{1}{4}} \tag{17}$$

For a given U_1, U_L, and U_s, the value of U_{2_opt} can be obtained according to Eq. (17).

4. METHOD OF PARAMETER OPTIMIZATION

In this section, a method of optimizing M_{12} and U_2 is proposed in order to obtain high efficiency and maintain output voltage constant. The process of the method of optimizing M_{12} (U_1) and U_2 is shown in Fig. 5.

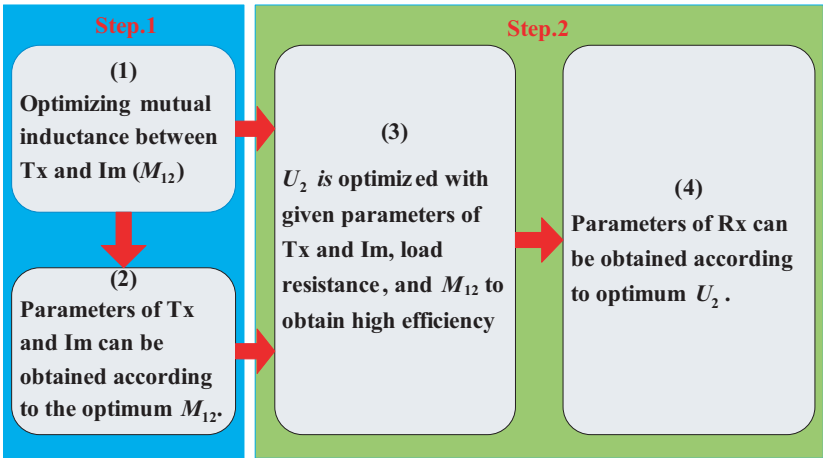

Figure 5. The process of the method of optimizing M_{12} and U_2.

Step 1. Optimizing M_{12}: M_{12} may be constant in the proposed structure to optimize the outer diameters and the numbers of turns of Tx and Im with misalignments. According to the optimum M_{12}, parameters of Tx and Im (diameters of Tx and Im, the numbers of turns of Tx and Im) can be obtained.

Step 2. Optimizing U_2: U_1, U_L, and U_s can be obtained according to the optimum M_{12}, optimum parameters of Tx and Im (diameters, turns), and the load resistance. The value of U_{2_opt} can be obtained according to Eq. (17). The outer diameter of Rx and the number of turns of Rx are optimized in order to obtain U_{2_opt}.

4.1. Optimizing M_{12}

It can be seen from Eq. (15) that the output voltage V_L is dependent on U_1, U_2, U_L, U_s, and $(R_3/R_1)^{1/2}$. In general, U_1, U_2, U_L, U_s, and $(R_3/R_1)^{1/2}$ are nearly constant when the parameters (R, L, C) of each coil and the load are given. However, The mutual inductance M_{12} may be changed with the variations of lateral misalignments (The variations of M_{12} result in the changes of U_1 and U_2, respectively). Lateral misalignments between Im and Rx may not occur, and M_{23} may be kept constant when both Im and Rx are fixed at the same plane by using the proposed structure. Lateral misalignments between Tx and Im or Rx may occur. Therefore, how to maintain the mutual inductance M_{12} (or U_1) constant is a problem. In this section, the method of the mutual inductance optimization is proposed. The mutual inductance M_{12} (or U_1) can be kept nearly constant with lateral misalignments by using the proposed method.

The process of the method of mutual inductance optimization is as follows:

1) Parameters setting: the resonant frequency is set to 85 kHz. The mutual inductance between the transmission coil and intermediate coil should be large enough to obtain high efficiency. The mutual inductance is set to 6.0 µH. The transmission distance is set to 15 cm. The diameter of copper is set to 2.3 mm. The outer diameter of Tx is changed from 0.25 m to 0.30 m in a step of 2.0 mm. The outer diameter of Im is changed from 0.2 m to 0.25 m in a step of 2.0 mm. The number of turns of Tx is changed from 17 to 40 in a step of 1. The number of turns of Im is changed from 6 to 10 in a step of 1.

2) Calculated mutual inductance: According to Eqs. (1) and (2), the mutual inductance between Tx and Im can be obtained with different lateral misalignments. M_{1210} is the mutual inductance between Tx and Im when lateral misalignment equals 10 cm; M_{120} is the mutual inductance between Tx and Im when lateral misalignment equals 0 cm.

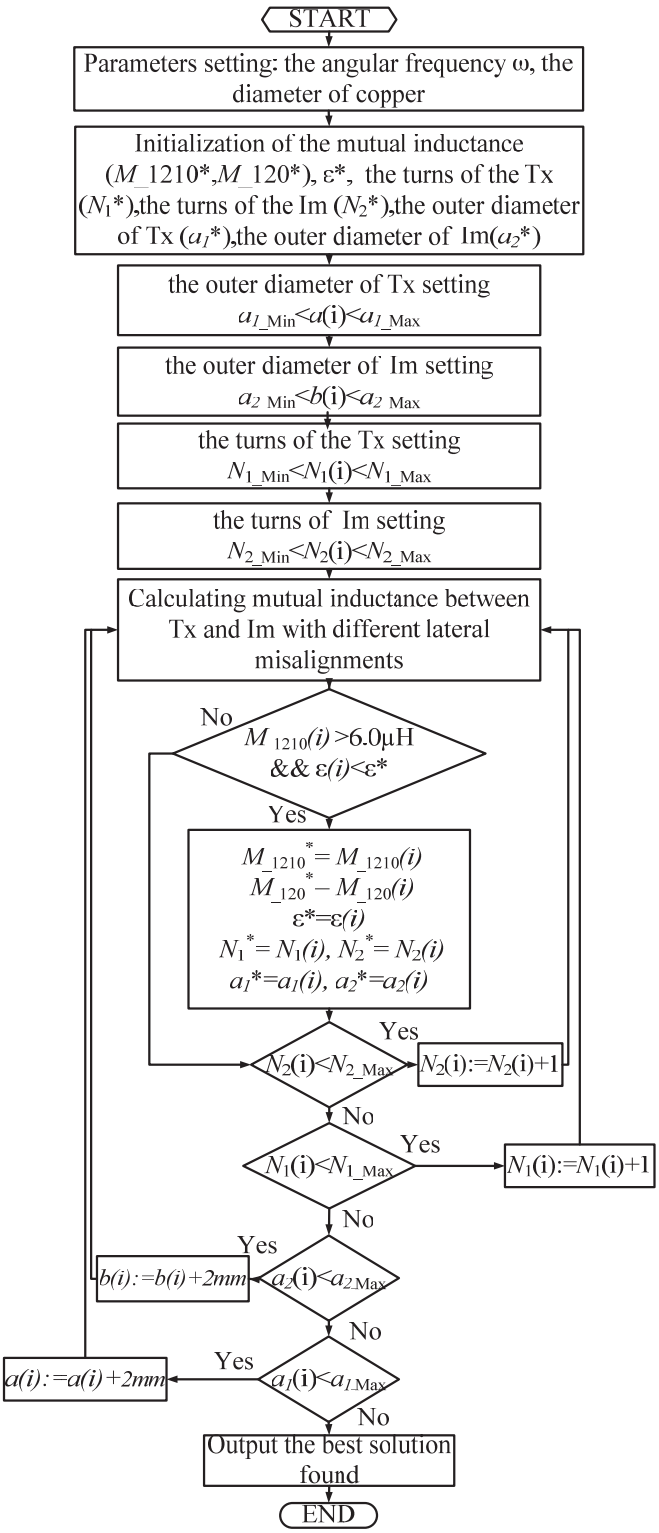

Figure 6. The flowchart of the method of the mutual inductance optimization.

3) Compared to ε ($\varepsilon = (M_{120} - M_{1210})/M_{120}$) at a given outer diameter of Tx, outer diameter of Im, the number of turns of Tx, and the number of turns of Im, the optimum ε is obtained (The smaller ε is, the smaller the variations of mutual inductance become).

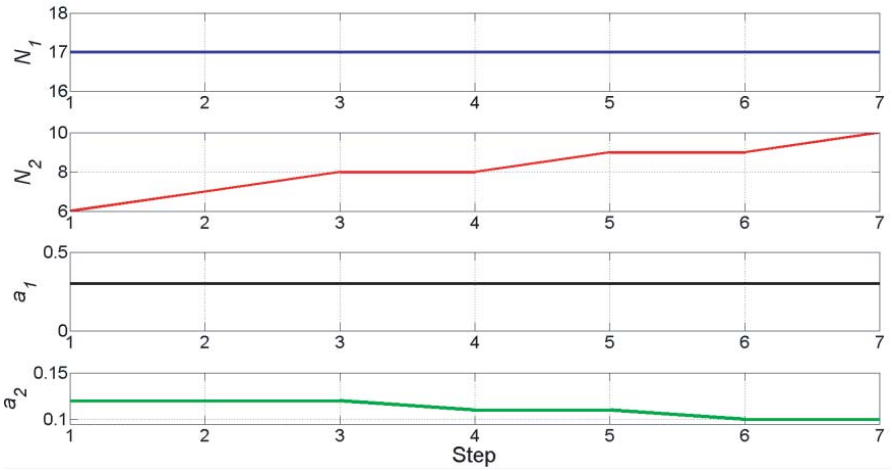

Figure 7. The optimum parameters of each coil. N_1 is the the number of turns of Tx, N_2 is the number of turns of Im, a_1 is the out radius of Tx, a_2 is the out radius of Im.

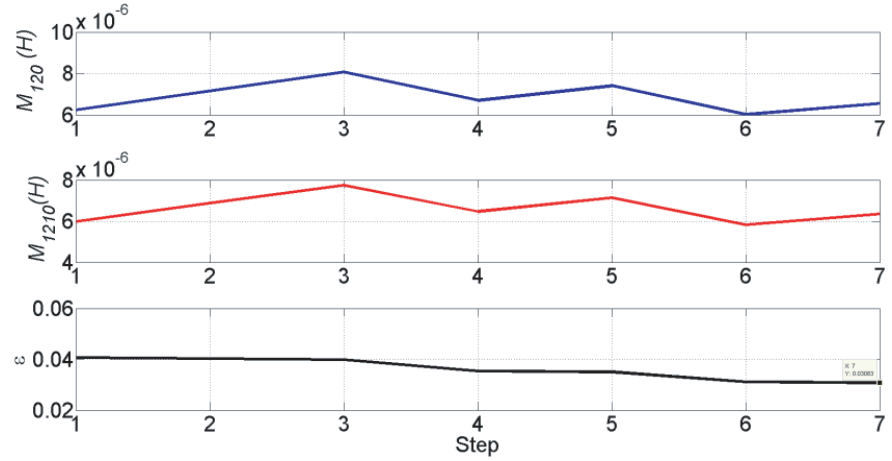

Figure 8. The optimum mutual inductance M_{120}, M_{1210} and ε.

4) According to the optimum ε, optimum parameters of Tx and Im can be obtained. The detailed optimization process is shown in Fig. 6.

Figure 7 shows optimum parameters of each coil (N_1, N_2, a, b). It can be seen that optimum N_1 is equal to 17, optimum N_2 equal to 10, optimum a_1 equal to 0.3 m, and optimum a_2 equal to 0.1 m. Fig. 8 shows optimum mutual inductance M_{120}, M_{1210}, and ε. It is clearly seen that all ε are smaller than 5%;optimum ε is 3.1%; all mutual inductances are larger than 6.0 µH. In the above analysis, it can be seen that the radius of Im should be decreased, and the number of turns of Im should be increased in order to obtain constant mutual inductance.

4.2. Optimizing U_2

U_2 is also a key parameter to obtain high efficiency, and optimum U_2 can be obtained by Eq. (17) with given U_1, U_L, and U_s. Parameters of Rx (the number of turns of Rx N_3 and the outer diameter of Rx a_3) can be obtained according to optimum U_2.

The process of the method of optimizing U_2 is as follows: 1) Parameters setting: the resonant frequency is set to 85 kHz. The diameter of copper is set to 2.3 mm. Optimum N_1 is set to 17, optimum N_2 set to 10, optimum a_1 set to 0.3 m, and optimum a_2 set to 0.1 m. The outer diameter of Rx is changed from 0.01 m to 0.10 m in a step of 2.0 mm. The number of turns of Rx is changed from 5 to 20

in a step of 1 turn (The diameter of each turn is 2.3 mm).

2) Calculate strong-coupling parameters U_2:

a) According to Eqs. (1)–(3), the mutual inductance between Im and Rx (M_{12}) can be obtained.

b) The self-inductances of Tx, Im, and Rx can be obtained according to Eqs. (3) and (4).

c) The coupling coefficients (k_{12} and k_{13}) can be obtained according to Eq. (5).

d) The resistances of Tx, Im, and Rx can be obtained according to Eq. (6).

e) The unload quality factors of Tx, Im, and Rx can be obtained according to $Q_1 = \omega L_1/R_1$, $Q_2 = \omega L_2/R_2$, and $Q_3 = \omega L_3/R_3$.

f) U_2 can be obtained according to $U_2 = k_{23}(Q_2Q_3)^{1/2}$.

3) Compare ε_1 with $\varepsilon_1^*(\varepsilon_1 = (U_2^* - U_2)/U_2^*)$ at a given outer diameter of Rx and the number of turns of Rx. The optimum ε_1 can be obtained.

4) According to optimum ε_1, optimum parameters of Rx can be obtained. The detailed optimization process is shown in Fig. 9.

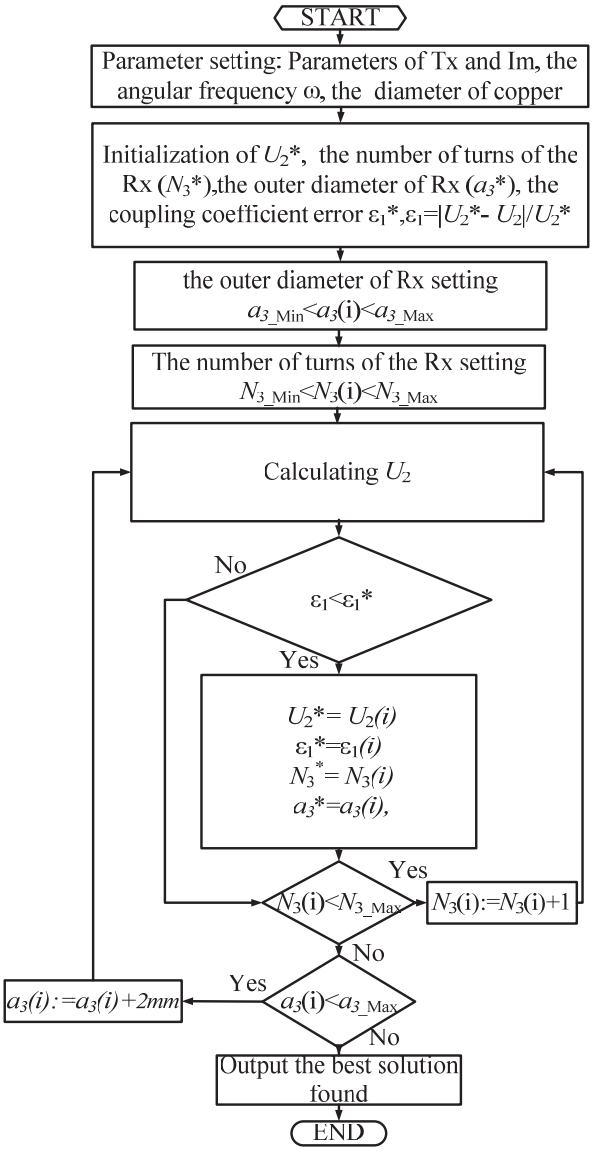

Figure 9. The flowchart of the method of optimization U_2.

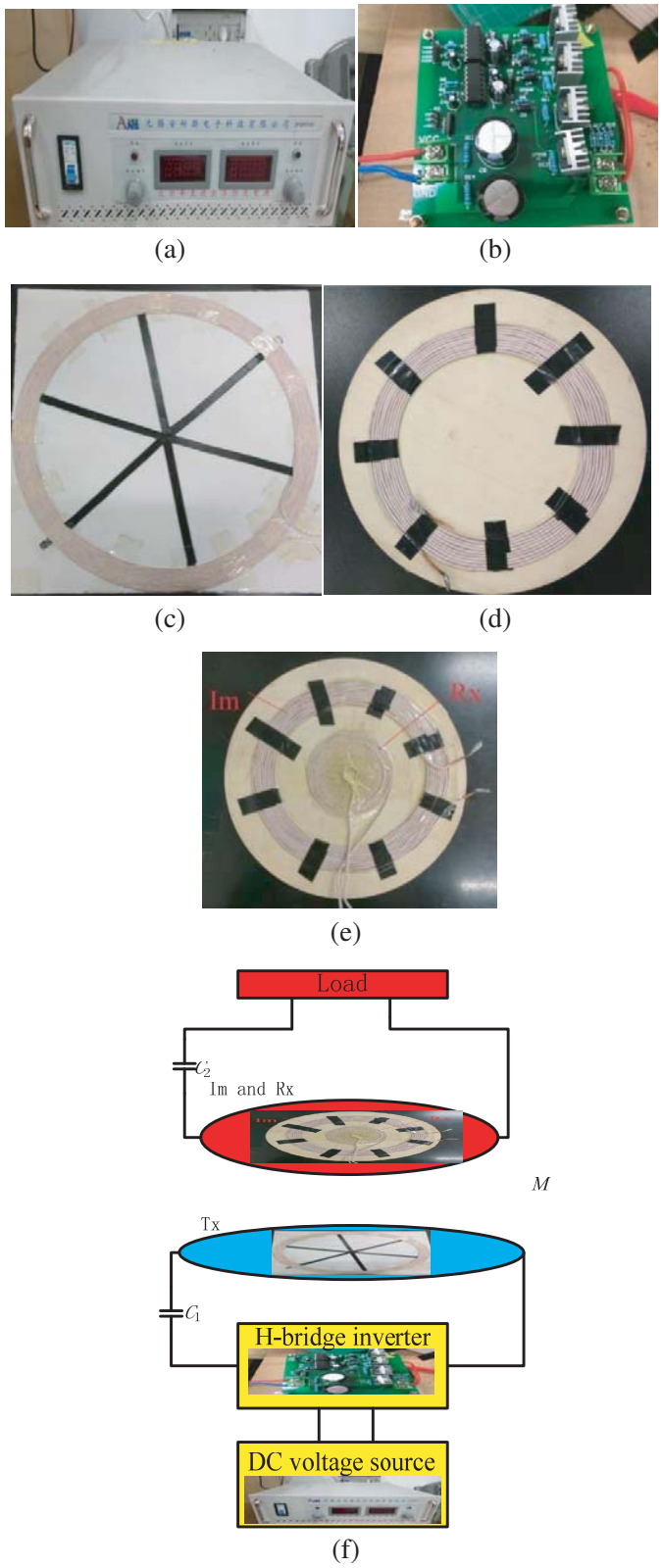

Figure 10. Experimental setup. (a) DC voltage source. (b) H-bridge inverter. (c) Tx. (d) Im. (e) Rx and Im. (f) The overall setup.

5. EXPERIMENTAL AND SIMULATION RESULTS

5.1. Experimental Setup

To validate the proposed structure and optimization method, the prototype model of the system has been built, as shown in Fig. 10. It is composed of a DC voltage source, a transmission resonant coil, an intermediate coil, a receiving resonant coil, an H-bridge inverter, and the load. The value of the DC voltage source is 36 V. The DC voltage source is shown in Fig. 10(a). H-bridge inverter is used at the transmitter side to provide AC excitation, as shown in Fig. 10(b). It contains four MOSFETs (IRF3207). The transmission resonant coil is shown in Fig. 10(c). The intermediate resonant coil is shown in Fig. 10(d). The intermediate resonant coil and receiving resonant coil are shown in Fig. 10(e). According to the optimization method, the outer diameter of the transmission resonant coil is 0.6 m with a pitch of 0 cm for approximately 17 turns; the outer diameter of intermediate resonant coil is 0.2 m with a pitch of 0 cm for approximately 10 turns; the outer diameter of receiving resonant coil is 0.09 m with a pitch of 0 cm for approximately 16 turns. All coils are made from 300-strand AWG 38Litz-wire.

Table 1. Measured parameters of the resonant coils.

Symbol	Parameter	Value
L_1	the inductance of Tx	333.7 µH
L_2	the inductance of Im	30.5 µH
L_3	the inductance of Rx	10.9 µH
C_1	the compensation capacitance of Tx	10.5 nF
C_2	the compensation capacitance of Im	115.0 nF
C_3	the compensation capacitance of Rx	321.6 nF
R_1	the parasitic resistance of Tx	0.402 Ω
R_2	the parasitic resistance of Im	0.067 Ω
R_3	the parasitic resistance of Rx	0.04 Ω
f_0	the original resonant frequency	85.0 kHz

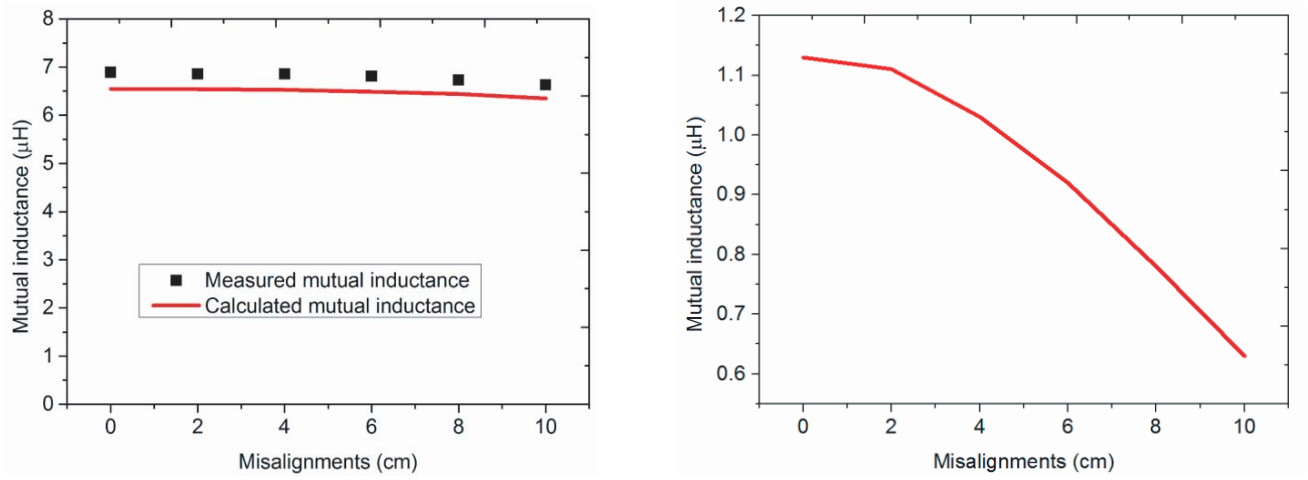

Figure 11. Measured and calculated mutual inductance versus misalignments with the proposed structure and the traditional structure. (a) Measured and calculated mutual inductance with proposed structure. (b) Measured and calculated mutual inductance with traditional structure.

An impedance analyzer is used to extract the parameters in Eqs. (7) and (8). The original resonant frequency is set to 85.0 kHz. The load resistance is set to 3.7 Ω with a tower-type coil WPT system. The transmission distance is 15 cm. Parameters of the resonant coils are listed in Table 1. The moving direction of the receiver is noted as y-axis, and the coordinates are marked in Fig. 2(b).

Figure 11(a) shows the measured and calculated mutual inductances between Tx and Im versus misalignments with the proposed structure. It can be seen that the mutual inductance between Tx and Im (M_{12}) is changed from 6.89 μH to 6.63 μH as the misalignment is varied from 0 cm to 10 cm. The difference between M_{120} and M_{1210} is 0.26 μH. ε is equal to 3.77% according to $\varepsilon = (M_{120} - M_{1210})/M_{120}$. The variations of mutual inductance are very smooth as the misalignment is varied from 0 cm to 10 cm. Fig. 11(b) shows the calculated mutual inductance between the transmission coil and receiving coil versus misalignments with the traditional structure (Both the transmission coil and receiving coil are the same as Im in size). It can be seen that the mutual inductance between the transmission coil and receiving coil is changed from 1.13 μH to 0.63 μH as the misalignment is varied from 0 cm to 10 cm. ε is equal to 44.24%. The variations of mutual inductance with the proposed structure are smaller than those of the traditional structure.

5.2. Two-Coil Structure

In the two-coil WPT system, Tx is the transmission coil, and Im is used as receiving coil. The load resistance is set to 10 Ω in order to obtain the optimum efficiency [11], and the value of the DC voltage source is set to 48 V.

Figure 12 shows the measured and calculated output voltages versus misalignments with the two-coil WPT system. It can be seen that the output voltage is changed from 14.40 V to 14.60 V as the misalignment is varied from 0 cm to 10 cm. The output voltage is nearly constant as misalignment is varied from 0 cm to 10 cm. Fig. 13 shows the measured and calculated efficiencies versus misalignments with the two-coil WPT system. It can be seen that the efficiency is changed from 65.6% to 63.5% as the misalignment is varied from 0 cm to 10 cm. The efficiency is also nearly constant as the misalignment is varied from 0 cm to 10 cm.

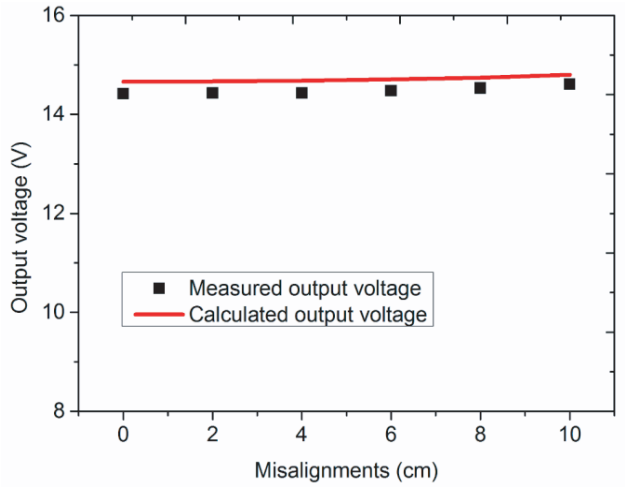

Figure 12. Measured and calculated output voltage versus misalignments.

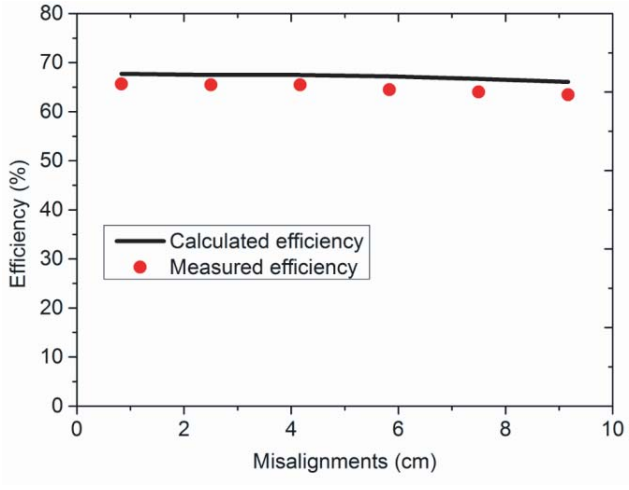

Figure 13. Measured and calculated efficiency versus misalignments with two-coil WPT system.

5.3. Structure of Tower-Type Coils

All parameters of the tower-type coil system are shown in Table 1 and Fig. 11. The strong-coupling parameter between Im and Rx U_2 can be obtained according to $U_2 = k_{23}(Q_2Q_3)^{1/2}$, and the actual U_2 is equal to 34.2. Optimum U_2 can also be calculated in terms of Eq. (17), and optimum U_2 equals 36.9. The value of actual U_2 is very close to the value of optimum U_2.

The effect of M_{13} (U_{13}) on the output voltage and efficiency is small in this paper according to the following calculated results. In order to analyse the effect of M_{13} (U_{13}) on the output voltage and efficiency, the calculated results can be obtained with the help of MATLAB in terms of Eqs. (12)–(16). Fig. 14(a) shows the calculated output voltage with considering M_{13} and without considering M_{13}. The output voltage with considering M_{13} is changed from 14.46 V to 15.79 V as the misalignment is varied from 0 cm to 12 cm. The output voltage without considering M_{13} is changed from 15.13 V to 16.24 V as the misalignment is varied from 0 cm to 12 cm. The value of the output voltage with considering M_{13} is nearly the same as that without considering M_{13}. Fig. 14(b) shows the calculated efficiency with considering M_{13} and without considering M_{13}. The efficiency with considering M_{13} is changed from 87.5% to 86.8% as the misalignment is varied from 0 cm to 12 cm. The efficiency with considering M_{13} is changed from 87.0% to 86.4% as the misalignment is varied from 0 cm to 12 cm. The value of the efficiency with considering M_{13} is also nearly the same as that without considering M_{13}.

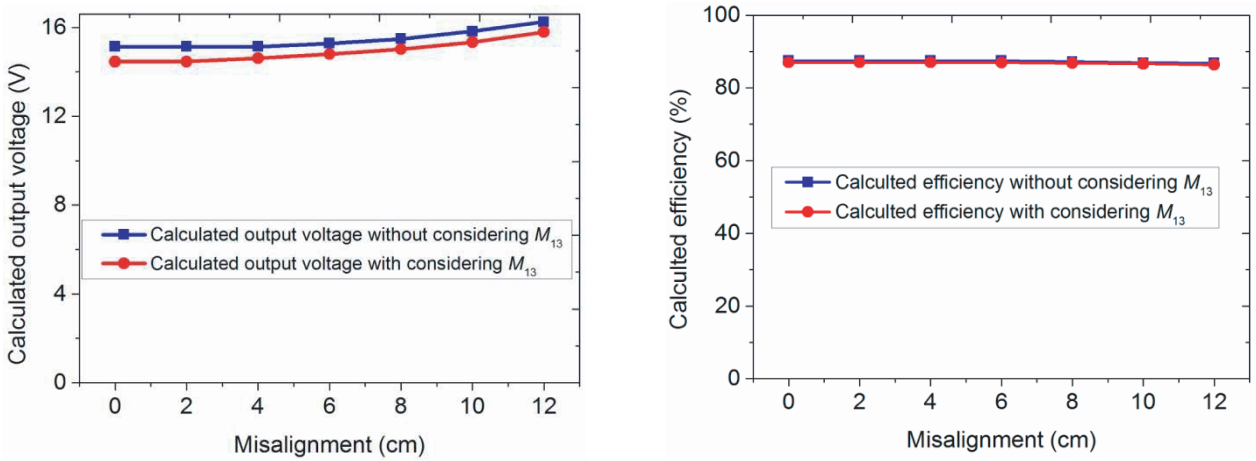

(a) (b)

Figure 14. Calculated output voltage and efficiency versus misalignments. (a) Calculated output voltage versus misalignments. (b) Calculated efficiency versus misalignments.

The misalignment Δ is set to 0 cm, 2 cm, 4 cm, 6 cm, 8 cm, 10 cm, and 12 cm, respectively. We test the input voltage, input current, the current of Im, and output voltage, respectively. Fig. 15 shows measured and calculated input currents versus misalignments. It can be seen that the input current is changed from 1.76 A to 1.89 A as the misalignment is varied from 0 cm to 12 cm. The input current of ratio of change is only 6.8%. It is convenient to design the transmission coil because the input current of ratio of change is small.

Figure 16 shows measured and calculated currents of Im versus misalignments. It can be seen that the current of Im is changed from 8.62 A to 9.02 A as the misalignment is varied from 0 cm to 12 cm. Compared with the value of the input current, the value of the current of Im is higher. This is beneficial for increasing the magnetic field strength of the Im coil. Therefore, the efficiency may be improved. And it is helpful for reducing the MOSFET of current stress.

Figure 17 shows the measured and calculated output voltages versus misalignments. It can be seen that the output voltage is changed from 14.07 V to 14.36 V as the misalignment is varied from 0 cm to 12 cm. The output voltage is nearly constant as the misalignment is varied from 0 cm to 12 cm. Fig. 18 shows the measured and calculated efficiencies versus misalignments. It can be seen that the efficiency is changed from 82.9% to 80.4% as the misalignment is varied from 0 cm to 12 cm. The output voltage and efficiency are nearly constant because the mutual inductance between Tx and Im (M_{12}) is nearly constant as the misalignment is varied from 0 cm to 12 cm. Compared to a two-coil structure, the efficiency of the structure of tower-type coils is higher because the magnetic field strength is increased when Im coil is added into the WPT system. The validity of the proposed method is verified by simulated and experimental results. Performance comparison between other references and our paper is shown in Table 2. Compared with lateral misalignments in references [14, 15, 18], lateral

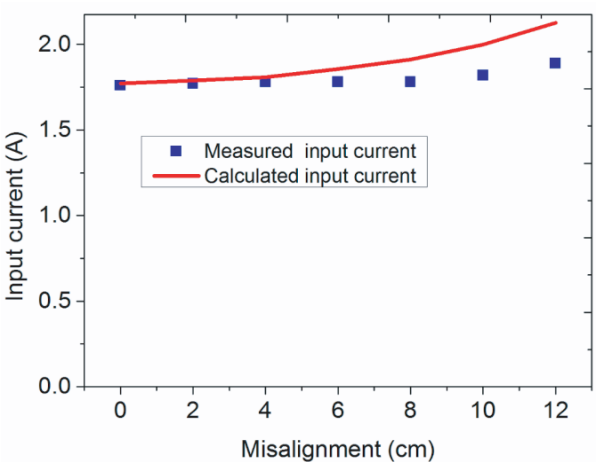

Figure 15. Measured and calculated input current versus misalignments.

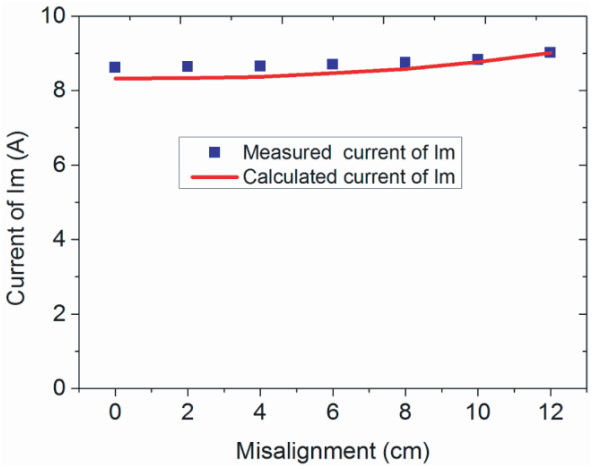

Figure 16. Measured and calculated current of Im versus misalignments.

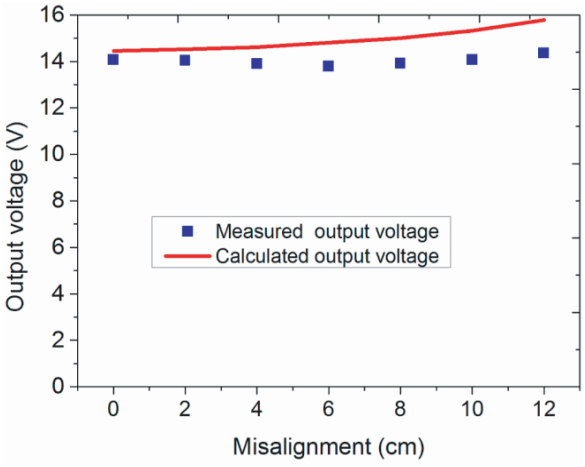

Figure 17. Measured and calculated output voltage versus misalignments.

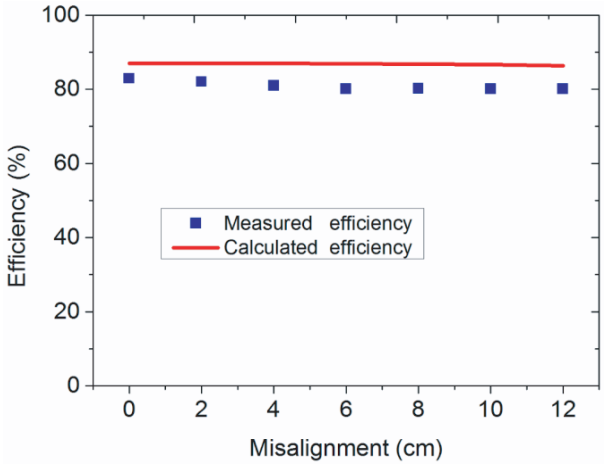

Figure 18. Measured and calculated efficiency versus misalignments.

Table 2. Performance comparison.

References	Size of Tx (Length ×width)	Size of Rx (Length ×width)	Lateral misalignments (cm)	Ratio of output power (%)	Ratio of efficiency (%)	Maximum efficiency (%)
[14]	30 cm × 20 cm	100 cm × 80 cm	X-direction: 24 Y-direction: /	50.0	30.0	74.0
[15]	20 cm × 10 cm	100 cm × 80 cm	X-direction: 30 Y-direction: 15	50.0	30.1	71.0
[18]	110 cm × 90 cm	70 cm × 20 cm	X-direction: 39 Y-direction: 18	29	/	/
[Our work]	Radius: 30 cm	Radius: 4.5 cm	X-direction: 12 Y-direction: 12	2.0	3.0	82.9

'/' denotes that the value is not given in reference.

misalignment is not the largest in this paper. However, the sizes of Tx and Rx are the smallest; the change rates of efficiency and power are the smallest; the misalignment of X-direction is the same as that of Y-direction; and the output voltage is kept nearly constant without the voltage regulator with misalignments. According to SAE J2954 standard, the misalignment in X direction is 10 cm, and the misalignment in Y direction is 7.5 cm. Therefore, the misalignments in both X and Y directions meet SAE J2954 standard by using the structure of tower-type coils.

6. CONCLUSION

In this paper, a structure of tower-type coils is proposed. The mathematical model of the proposed structure with lateral misalignments is built based on equivalent circuit method. The mutual inductance between the transmission coil and intermediate coil is kept nearly constant as the misalignment is varied from 0 cm to 12 cm, and the optimum strong-coupling parameter U_2 is also obtained according to the proposed optimization method. Both the output voltage and efficiency are nearly constant with different lateral misalignments by using the proposed structure and method. Experimental results show that the mutual inductance of the transmission coil and intermediate coil is changed from 6.88 µH to 6.63 µH, the output voltage ranged from 14.07 V to 14.36 V, and the efficiency changed from 82.9% to 80.4% as the misalignment is varied from 0 cm to 12 cm in the tower-type coil WPT system. We will further increase the lateral misalignments to meet the needs of the dynamic wireless power transfer system.

ACKNOWLEDGMENT

This work was supported in part by the National Natural Science Foundation of China under Grant 51377001, in part by the Hunan Provincial Department of Education under Grant17C0469, in part by Hunan Provincial Natural Science Foundation of China under Grant 2018JJ3127, in part by Zhuzhou City Natural Science Foundation of China.

REFERENCES

1. Musavi, F. and W. Eberle, "Overview of wireless power transfer technologies for electric vehicle battery charging," *IET Power Electronics*, Vol. 7, 60–66, 2014.
2. Mi, C. C., G. Buja, S. Y. Choi, and C. T. Rim, "Modern advances in wireless power transfer systems for roadway powered electric vehicles," *IEEE Transactions on Industrial Electronics*, Vol. 63, 6533–6545, 2016.
3. Li, J., Y. Lu, F. Liu, B. Mu, Z. Dong, S. Pan, and C. Zheng, "Optimization method of magnetic coupling resonant wireless power transfer system with single relay coil," *Progress In Electromagnetics Research M*, Vol. 80, 57–70, 2019.
4. Liu, B. J., H. T. Xu, and X. W. Zhou, "Resource allocation in wireless-powered mobile edge computing systems for internet of things applications," *Electronics*, Vol. 8, No. 2, 206, Feb. 2019.
5. Choi, S. Y., B. W. Gu, S. Y. Jeong, and C. T. Rim, "Advances in wireless power transfer systems for roadway-powered electric vehicles," *IEEE Journal of Emerging and Selected Topics in Power Electronics*, Vol. 3, 18–36, 2015.
6. Li, Z., C. Zhu, J. Jiang, K. Song, and G. Wei, "A 3-kW wireless power transfer system for sightseeing car supercapacitor charge," *IEEE Transactions on Power Electronics*, Vol. 32, 3301–3316, 2017.
7. Wang, T. F., X. Liu, N. Jin, H. J. Tang, X. J. Yang, and M. Ali, "Wireless power transfer for battery powering system," *Electronics*, Vol. 7, No. 9, 178, Sep. 2018.
8. Zhang, Y., K. Chen, F. He, Z. Zhao, T. Lu, and L. Yuan, "Closed-form oriented modeling and analysis of wireless power transfer system with constant-voltage source and load," *IEEE Transactions on Power Electronics*, Vol. 31, 3472–3481, 2016.
9. Huang, S., Z. Li, Y. Li, X. Yuan, and S. Cheng, "A comparative study between novel and conventional four-resonator coil structures in wireless power transfer," *IEEE Transactions on Magnetics*, Vol. 50, 1–4, 2014.

10. Fotopoulou, K. and B. W. Flynn, "Wireless power transfer in loosely coupled links: Coil misalignment model," *IEEE Transactions on Magnetics*, Vol. 47, 416–430, 2011.
11. Wang, J., J. Li, S. L. Ho, W. N. Fu, Y. Li, H. Yu, and M. Sun, "Lateral and angular misalignments analysis of a new PCB circular spiral resonant wireless charger," *IEEE Transactions on Magnetics*, Vol. 48, 4522–4525, 2012.
12. Huang, S. D., Z. Q. Li, and Y. Li, "Transfer efficiency analysis of magnetic resonance wireless power transfer with intermediate resonant coil," *Journal of Applied Physics*, Vol. 115, May 7, 2014.
13. Zhang, Y., T. Lu, Z. Zhao, F. He, K. Chen, and L. Yuan, "Employing load coils for multiple loads of resonant wireless power transfer," *IEEE Transactions on Power Electronics*, Vol. 30, 6174–6181, 2015.
14. Zhang, Y., T. Lu, Z. Zhao, K. Chen, F. He, and L. Yuan, "Wireless power transfer to multiple loads over various distances using relay resonators," *IEEE Microwave and Wireless Components Letters*, Vol. 25, 337–339, 2015.
15. Li, H., J. Li, K. Wang, W. Chen, and X. Yang, "A maximum efficiency point tracking control scheme for wireless power transfer systems using magnetic resonant coupling," *IEEE Transactions on Power Electronics*, Vol. 30, 3998–4008, 2015.
16. Huh, J., S. W. Lee, W. Y. Lee, G. H. Cho, and C. T. Rim, "Narrow-width inductive power transfer system for online electrical vehicles," *IEEE Transactions on Power Electronics*, Vol. 26, 3666–3679, 2011.
17. Choi, S. Y., S. Y. Jeong, B. W. Gu, G. C. Lim, and C. T. Rim, "Ultraslim S-type power supply rails for roadway-powered electric vehicles," *IEEE Transactions on Power Electronics*, Vol. 30, 6456–6468, 2015.
18. Waffenschmidt, E., "Homogeneous magnetic coupling for free positioning in an inductive wireless power system," *IEEE Journal of Emerging and Selected Topics in Power Electronics*, Vol. 3, 226–233, 2015.
19. Zhang, Z. and K. T. Chau, "Homogeneous wireless power transfer for move-and-charge," *IEEE Transactions on Power Electronics*, Vol. 30, 6213–6220, 2015.
20. Su, Y. C., H. Jin, W. Y. Lee, and C. T. Rim, "Asymmetric coil sets for wireless stationary EV chargers with large lateral tolerance by dominant field analysis," *IEEE Transactions on Power Electronics*, Vol. 29, 6406–6420, 2014.
21. Ram Rakhyani, A. K., S. Mirabbasi, and M. Chiao, "Design and optimization of resonance-based efficient wireless power delivery systems for biomedical implants," *IEEE Transactions on Biomedical Circuits and Systems*, Vol. 5, 48–63, 2011.
22. Soma, M., D. C. Galbraith, and R. L. White, "Radio-frequency coils in implantable devices: misalignment analysis and design procedure," *IEEE Transactions on Biomedical Engineering*, Vol. 34, 276–282, 1987.
23. Zierhofer, C. M. and E. S. Hochmair, "Geometric approach for coupling enhancement of magnetically coupled coils," *IEEE Transactions on Biomedical Engineering*, Vol. 43, 708–714, 1996.
24. Ke, Q., W. Luo, G. Yan, and K. Yang, "Analytical model and optimized design of power transmitting coil for inductively coupled endoscope robot," *IEEE Transactions on Biomedical Engineering*, Vol. 63, 694–706, 2016.